Hydrophobic Mutations Alter the Movement of Mg^{2+} in the Pore of Voltage-Gated Potassium Channels

Richard E. Harris and Ehud Y. Isacoff
Department of Molecular and Cell Biology, Division of Neurobiology, University of California, Berkeley, California 94720 USA

ABSTRACT The permeation pathways of the voltage-gated K^+ channels Kv3.1 and ShakerB Δ6–46 (ShBΔ) were studied using Mg^{2+} block. Internal Mg^{2+} blocked both channels in a voltage-dependent manner, and block was partially relieved by external K^+, consistent with Mg^{2+} binding within the pore. The kinetics of Mg^{2+} block was much faster for Kv3.1 than for ShBΔ. Fast block of Kv3.1 was transferred to ShBΔ with transplantation of the P-region, but not of S6. The difference in the P-region, causing the change in Mg^{2+} binding kinetics, was attributed to ShBΔ(V443) and its analog Kv3.1(L401), because in both channels leucine at this position gave fast block, whereas valine gave slow block. For Kv3.1 the major determinant of the voltage dependence of Mg^{2+} binding resided primarily in the off rate, whereas for Kv3.1(L401V) the voltage dependence resided primarily in the on rate, consistent with a change in the rate-limiting barrier for Mg^{2+} binding. Our data suggest that hydrophobic residues at positions 401 of Kv3.1 and 443 of ShBΔ act as barriers to the movement of Mg^{2+} in the pore.

INTRODUCTION

K^+ channels are thought to have long pores that can be simultaneously occupied by multiple permeant ions fluxing in single file (Hille, 1992). During flux, ions are thought to squeeze through a narrow passage, exchanging interactions with water for interactions with pore-lining residues that form ion-binding sites and barriers to ion movement. Attempts to identify pore-lining residues have provided evidence that the S4-S5 loop and S6 contribute to the internal vestibule of the pore (Choi et al., 1993; Isacoff et al., 1991; Slesinger et al., 1993; Lopez et al., 1994; Taglialatela et al., 1994a), and that the S5-S6 loop forms the external vestibule (MacKinnon and Miller, 1989; MacKinnon et al., 1990; Heginbotham and MacKinnon, 1992a; Goldstein et al., 1994; Hidalgo and MacKinnon, 1995; Aiyar et al., 1995) and the narrowest portion of the pore (Lu and Miller, 1995; Pascual et al., 1995; Kurz et al., 1995), where ion selectivity is determined (MacKinnon and Yellen, 1990; Yool and Schwarz, 1991; Heginbotham et al., 1992b; Taglialatela et al., 1993; Heginbotham et al., 1994). Owing to the high rate of flux and multiple occupancy of permeant ions, it has not been possible to dissect ion entry, pore binding, and ion exit, making it difficult to answer some of the most basic questions about the nature of pore-ion interactions. This problem has been solved with the blocking ions Ba^{2+} (Armstrong et al., 1982; Neyton and Miller, 1988a,b) and Mg^{2+} (Matsuda, 1991; Lu and MacKinnon, 1994), which bind deep in the permeation pathway, and enter and exit the K^+ channel pore much more slowly than does K^+, making them excellent probes for studying the energetics of ion movement in the pore.

We focused on Mg^{2+} block of voltage-gated K^+ channels, about which little is known. We present here the first determination of the binding kinetics of internal Mg^{2+} for these channels. We found that Mg^{2+} blocks the voltage-gated K^+ channel Kv3.1 under physiological conditions. As observed with block of inward-rectifier K^+ channels (Matsuda et al., 1987), we found that Mg^{2+} binds deep within the permeation pathways of Kv3.1 and ShBΔ, and that a single ion is sufficient to produce block, confirming earlier results on Kv2.1 and RCK4 (Ludewig et al., 1993; Lopatin et al., 1994). However, unlike inward rectifiers, in which Mg^{2+} block is regulated by amino acids in and near M2 (Lu and MacKinnon, 1994, 1995; Stanfield et al., 1994; Taglialatela et al., 1994b; Yang et al., 1995)—the proposed structural analog of the voltage-gated K^+ channel S6 (Kubo et al., 1993)—we identified a residue in the most conserved selectivity region of the S5-S6 loop (the P-region or H5) as a major determinant of Mg^{2+} binding. Our results suggest that this residue, which appears to lie at the internal lip of the narrowest part of the pore (Pascual et al., 1995), acts as an energetic barrier to the movement of Mg^{2+} when it is a valine and prevents deeper penetration of Mg^{2+} in the pore when it is leucine.

MATERIALS AND METHODS

Molecular biology

Kv3.1 and ShBΔ genes had been cloned into pBluescript (Stratagene) − and + vectors, respectively. Plasmids were transformed into DH5α cells, and dsDNA was isolated by an alkaline lysis procedure. Mutant plasmids were generated by the *dut⁻ung⁻* procedure, as described by Sambrook et al. (1989). Three Kv3.1(L401V) clones were made, by separate mutagenesis reactions, to ensure that effects on Mg^{2+} block were specific for the 401 mutation and there were not spurious mutations elsewhere. Mutant plasmids were sequenced by the Sanger dideoxy method. Chimeric chan-

Received for publication 25 January 1996 and in final form 22 March 1996.

Address reprint requests to Dr. Ehud Y. Isacoff, Department of Molecular and Cell Biology, Division of Neurobiology, 229 Stanley Hall, University of California, Berkeley, CA 94720. Tel.: 510-642-9853; Fax: 510-643-9290; E-mail: ehud@uclink.berkeley.edu.

0006-3495/96/07/209/11 $2.00

nels were constructed by restriction digestion methodologies outlined by Sambrook et al. (1989). cRNA was prepared from mutant and wild-type plasmids by an in vitro runoff transcription reaction using either Ambion (Megascript) or Stratagene transcription kits. Kv3.1 and ShBΔ plasmids were linearized with *Not*I and *Hin*dIII, respectively, and cRNA was generated by using either T7 or T3 RNA polymerases. RNA pellets were resuspended in ultrapure water (Specialty Media, Lavallette, NJ), and yield was determined by formaldehyde-agarose gel electrophoresis. Aliquots were stored at −80°C until they were ready for oocyte injection.

Electrophysiology

Stage V and VI *Xenopus laevis* oocytes were isolated, collagenased (Worthington Biochemical Corp.), and stored at 18°C. After isolation, 50–100 nl of cRNA was injected into each oocyte, and recordings were made 2–6 days after injection.

Before recording, oocytes were devitelinized manually after a 2–5-min incubation in solution containing (in mM) 220 NaAsp, 10 HEPES (pH 7.1 with NaOH), 10 EGTA (pH 7.1 with NaOH), and 2 $MgCl_2$. Devitelinized oocytes were placed in a bath solution containing (in mM) 98 KCl (K^+ from HEPES and EGTA yields a final concentration of 102), 10 HEPES (pH 7.1 with KOH), 10 EGTA (pH 7.1 with KOH), and 0.5 $MgCl_2$. Electrodes (0.5–2 MΩ) were pulled, fire polished, and filled with either Na^+ or K^+ external solutions. Na^+ and K^+ external solutions contained (in mM) either 98 NaCl or 98 KCl (K^+ or Na^+ from HEPES yields a final concentration of 100), 10 HEPES (pH 7.1 with KOH or NaOH), 0.3 $CaCl_2$, and 1.5 $MgCl_2$. Pipettes were zeroed to the bath reference electrode, and gigaohm seals were made onto oocyte membranes, using little or no suction to prevent large amounts of membrane invagination. Inside-out patches were made by quick excision and perfused with internal solutions containing (in mM) 98 KCl (K^+ from HEPES and EGTA yields a final concentration of 102), 10 HEPES (pH 7.1 with KOH), 10 EGTA (pH 7.1 with KOH), and X mM free $MgCl_2$ (X = 0, 0.0961, 0.481, 1.93, 4.84, and 11.7). Free $MgCl_2$ concentrations were determined with the computer program MAXCHELATOR (Hopkins Marine Station, Pacific Grove, CA). For the internal solution containing 0 Mg^{2+}, 10 EGTA was replaced with 10 EDTA and no $MgCl_2$ was added. Patches were perfused with 0 Mg^{2+} internal solution quickly after excision to minimize rundown. All recordings were performed at 25°C.

Patches were held from −100 mV to −80 mV and stepped to test potentials at 0.1 Hz for macroscopic data and 0.25–1 Hz for single-channel recordings. The duration of test potentials was 15 ms for macroscopic recordings and 100–200 ms for single-channel recording. Because of pipette series resistance, no deviations from the command voltage greater than 5 mV occurred for macropatches. Leak currents were subtracted with a P/4 protocol for macropatches and off line with averaged blank traces for single-channel patches. Data were acquired using either a List EP7 or an Axopatch 200 A amplifier (Axon Instruments, Foster City, CA), an AD/DA converter TL-1 DMA interface, and an IBM 486 AST PC. Data were sampled at 5 or 20 kHz, filtered first at 10 kHz with either a 4-pole low-pass Bessel filter (Axopatch 200A) or a 2-pole low-pass Bessel filter (List EP7), and filtered again at either 1 or 4 kHz with a second low-pass, 8-pole Bessel filter (Frequency Devices). Data were analyzed with pClamp software (Axon Instruments).

Amplitude distribution analysis

Amplitude distribution analysis was carried out essentially as described by Yellen (1984a). Amplitude histograms were generated from single-channel openings (10–50 ms in duration) containing no closing events and normalized to have an area of 1. β-functions were generated using the following equation:

$$f(y) = [y^{a-1}(1-y)^{b-1}]/B(a,b), \quad (1)$$

where $a = a\tau$, $b = b\tau[Mg^{2+}]$, and $B(a,b) = \int_0^1 y^{a-1}(1-y)^{b-1}dy$. τ is $0.228/f_c$, where f_c is the −3-dB cutoff frequency of the 8-pole, low-pass Bessel filter. a and b are the off and on rates, respectively, of Mg^{2+}. Because open channel noise was significant, each β-function was convolved with a Gaussian, the standard deviation of which was that of the open-channel noise in the absence of Mg^{2+}. The convolved functions were then fit to the normalized amplitude distributions of data obtained in the presence of Mg^{2+}. Distributions were fit with a computer program that minimized χ^2.

RESULTS

Internal magnesium block of Kv3.1 and ShBΔ

To characterize the permeation pathway of voltage-dependent K^+ channels, we compared internal Mg^{2+} block of the Shaw and Shaker K^+ channel subfamily members, Kv3.1 and ShBΔ (Hoshi et al., 1990). Application of internal Mg^{2+} to inside-out macropatches containing Kv3.1 or ShBΔ blocked currents through both channels at depolarized potentials (Fig. 1, *A* and *B*). In both channels activation kinetics were unaltered by Mg^{2+}, and tail kinetics were slowed. The slowing of the tail kinetics suggests that Mg^{2+} must unbind before the channels can deactivate. Dose-response curves of both channels were described well with Langmuir isotherms without cooperativity, indicating that the binding of one Mg^{2+} ion to the channel is sufficient to block current.

The affinity and kinetics of Mg^{2+} block, however, differed markedly between these two channels. At the macroscopic level, Kv3.1 displayed a 10-fold higher affinity for Mg^{2+} than did ShBΔ ($p < 10^{-5}$) (Fig. 1 *C*). Block at the single-channel level differed between Kv3.1 and ShBΔ more dramatically than expected for a 10-fold difference in macroscopic Mg^{2+} affinity. In external K^+, Mg^{2+} blocking and unblocking events of ShBΔ could be resolved (Fig. 1 *E*). However, under the same conditions, Mg^{2+} block of Kv3.1 decreased single-channel current amplitude without producing observable block events or increasing open-channel noise (Fig. 1 *D*), indicating that Mg^{2+} on and off rates for binding were too fast to be resolved by the limited bandwidth of our recording system. The reduction by 0.5 mM Mg^{2+} of the open probability of ShBΔ was less than the fractional reduction of single-channel current amplitude of Kv3.1, in agreement with the greater Mg^{2+} affinity of Kv3.1 at the macroscopic level.

We set out to determine whether block by internal Mg^{2+} is due to binding in the pore, to find the molecular differences between ShBΔ and Kv3.1 that are responsible for the different binding kinetics, and to quantitate the voltage dependence of the on and off rates of internal Mg^{2+} to determine the difference in energy profiles for Mg^{2+} association and dissociation between these two channels.

Magnesium block is sensitive to both external potassium and voltage

Macroscopic block by internal Mg^{2+} was voltage dependent and was well described by the Woodhull model (Woodhull, 1973) (Fig. 2 *A*). The voltage dependence indicated a posi-

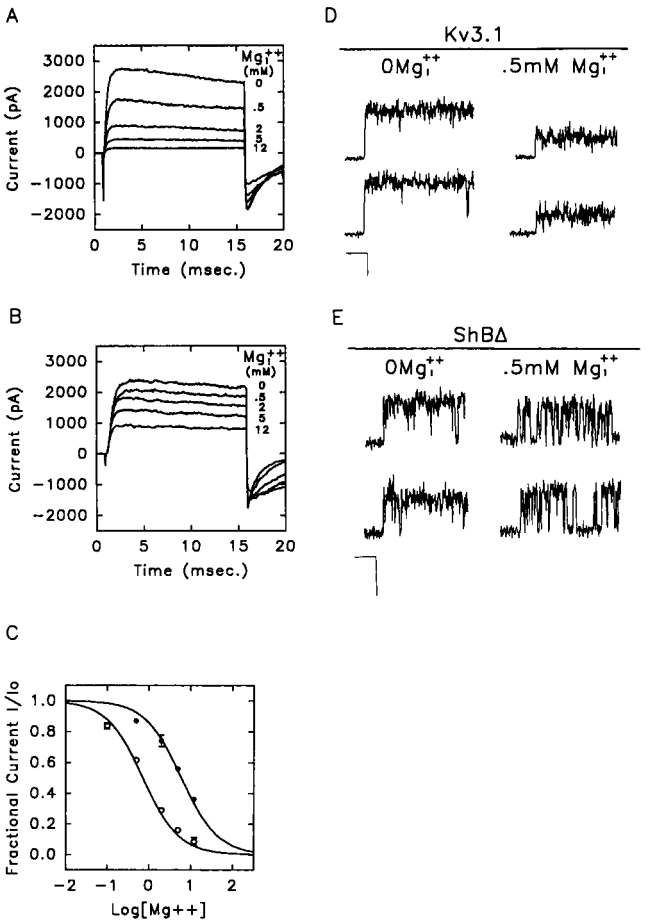

FIGURE 1 Internal Mg^{2+} block of Kv3.1 and ShBΔ with 100 mM K^+ out. (*A*) Kv3.1 and (*B*) ShBΔ inside-out macro patches perfused with internal magnesium at the listed concentrations. Step potential is +120 mV. (*C*) Internal Mg^{2+} dose-response curves for Kv3.1 (○) and ShBΔ (●). Current values were measured at steady state 3 to 5 ms after the depolarizing step. Fits are to the equation $I/I_o = 1/(1 + [Mg_i^{2+}]/K_i)$, with K_i equaling 0.80 ± 0.04 mM (n = 4) for Kv3.1 and 6.02 ± 0.49 mM (n = 4) for ShBΔ. (*D*) Kv3.1 and (*E*) ShBΔ single-channel currents with and without 0.5 mM Mg^{2+}_i. Step potential is +160 mV. Scale bars are 20 ms and 2 pA for both *D* and *E*.

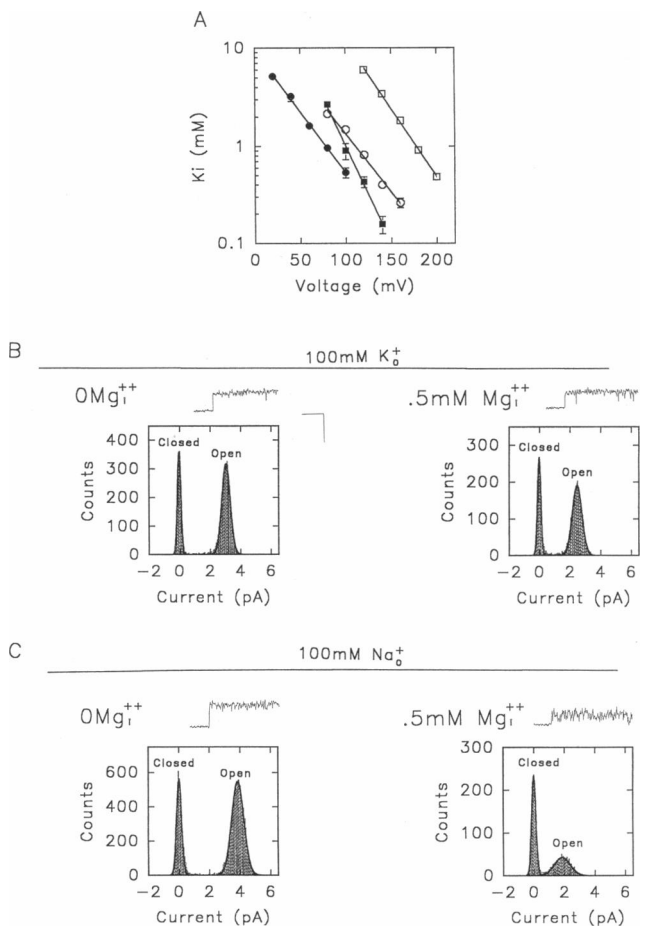

FIGURE 2 Influence of external K^+ on internal Mg^{2+} block. (*A*) Voltage dependence of K_i (Mg^{2+}) for Kv3.1 (○, ●) and ShBΔ (□, ■) from macroscopic currents as in Fig. 1 *C*. Filled symbols represent 100 mM Na_o^+, and open symbols represent 100 mM K_o^+. Fits are to the equation $K_i = K_{i0\ mV} * \exp - (FVZ\delta/RT)$. δ is the depth in the electric field of the binding site, $K_{i0\ mV}$ is the K_i with no applied voltage, and Z is 2 for the divalent Mg^{2+} ion. Values for depth in the electric field of the binding site (δ) are 0.37 (○), 0.40 (●), 0.41 (□), and 0.54 (■). $K_{i0\ mV}$ is (in mM) 26.15 ± 4.54 (n = 3) (○), 11.57 ± 1.06 (n = 5) (●), 307 ± 78.5 (n = 4) (□), and 78.1 ± 16.4 (n = 3) (■). (*B* and *C*) Single-channel traces and amplitude histograms for Kv3.1 with 100 mM K_o^+ and 100 mM Na_o^+. Mean single-channel current amplitude in Mg^{2+} decreases from 2.22 ± 0.11 pA (n = 5) to 1.90 ± 0.06 pA (n = 6) ($p < 0.03$) and standard deviation about the mean increases from 0.18 ± 0.01 pA (n = 5) to 0.41 ± 0.02 pA (n = 3) ($p < 0.0001$) when K^+ is substituted for Na^+. Step potential is +100 mV. Scale bars are 20 ms and 5 pA for both *B* and *C*.

tion in the membrane electric field of the Mg^{2+} ion-binding site (δ) of 0.37 for Kv3.1 and 0.41 for ShBΔ (from the inside) in the presence of external K^+. Substitution of external K^+ with Na^+ increased blocking affinity (decreased K_i) across the entire voltage range studied for both channels (Fig. 2 *A*). For Kv3.1, replacement of K_o^+ with Na_o^+ increased internal Mg^{2+} affinity by threefold ($p <$ 0.01) without altering the voltage dependence of Mg^{2+} binding. This observation is consistent with occupancy by external K^+ of a binding site that lies outside of the electric field that destabilizes the binding of Mg^{2+} by repulsion (Matsuda, 1991). In contrast to Kv3.1, substitution of K_o^+ with Na_o^+ increased the voltage dependence of Mg^{2+} block in ShBΔ from 0.40 to 0.54, revealing an important difference in Mg^{2+} block between the two channels (see below and Discussion). The "*trans* relief" by K^+ of block by internal Mg^{2+}, and the voltage dependence of the block, suggest strongly that the Mg^{2+} ion-binding site is located deep within the permeation pathways of both Kv3.1 and ShBΔ.

The increase in Mg^{2+} block after the removal of external K^+ was also evident at the single-channel level for Kv3.1 and was accompanied by an increase in open-channel noise (Fig. 2, *B* and *C*, *current traces*). Such an increase in open-channel noise is indicative of a slowing in blocking kinetics (Yellen, 1984b). The fact that the increased block is accompanied by an increase in noise suggests that removal of external K^+ slows the off rate of Mg^{2+} from its binding site.

Mutations in the P-region affect magnesium binding

To identify the molecular determinants of the different Mg^{2+} binding kinetics of Kv3.1 and ShBΔ, chimeric channels were constructed (Fig. 3 *B*). Transplantation of the S6 region of Kv3.1 into ShBΔ, ShBΔ[S6(Kv3.1)] increased single-channel current amplitude, as shown earlier (Lopez et al., 1994), without altering the Mg^{2+} blocking kinetics (Fig. 3 *A*). On the other hand, transplantation of the P-region from Kv3.1 into ShBΔ conferred on ShBΔ the fast blocking kinetics characteristic of Kv3.1: internal Mg^{2+} decreased single-channel current amplitude, increased open-channel noise, and eliminated resolvable block and unblock events in ShBΔ[P-region(Kv3.1)] channels (Fig. 3 *A*).

To narrow the specific portion of the P-region responsible for the effect of the transplantation, we focused on the only difference between these channels in the most conserved portion of the P-region, V443 of ShBΔ and the homologous L401 of Kv3.1 (Fig. 3 *B*). ShBΔ(V443L) channels exhibited the same fast Mg^{2+} blocking kinetics as the ShBΔ[P-region (Kv3.1)] chimeric channel and Kv3.1 (Fig. 3 *A*). The reciprocal mutation in Kv3.1, L401V, had the opposite effect, converting the fast block of Kv3.1 to the slow block characteristic of ShBΔ (Fig. 3 *A*). These reciprocal results indicate that the difference in Mg^{2+} binding between these two channels can be attributed to a single hydrophobic position in the highly conserved K^+ channel signature sequence of the P-region. Other pore properties such as single-channel conductance and K^+/Na^+ selectivity were normal in Kv3.1(L401V) channels.

Three other mutations at this position, Kv3.1(L401D, K, and A), failed to express as homomultimers, and

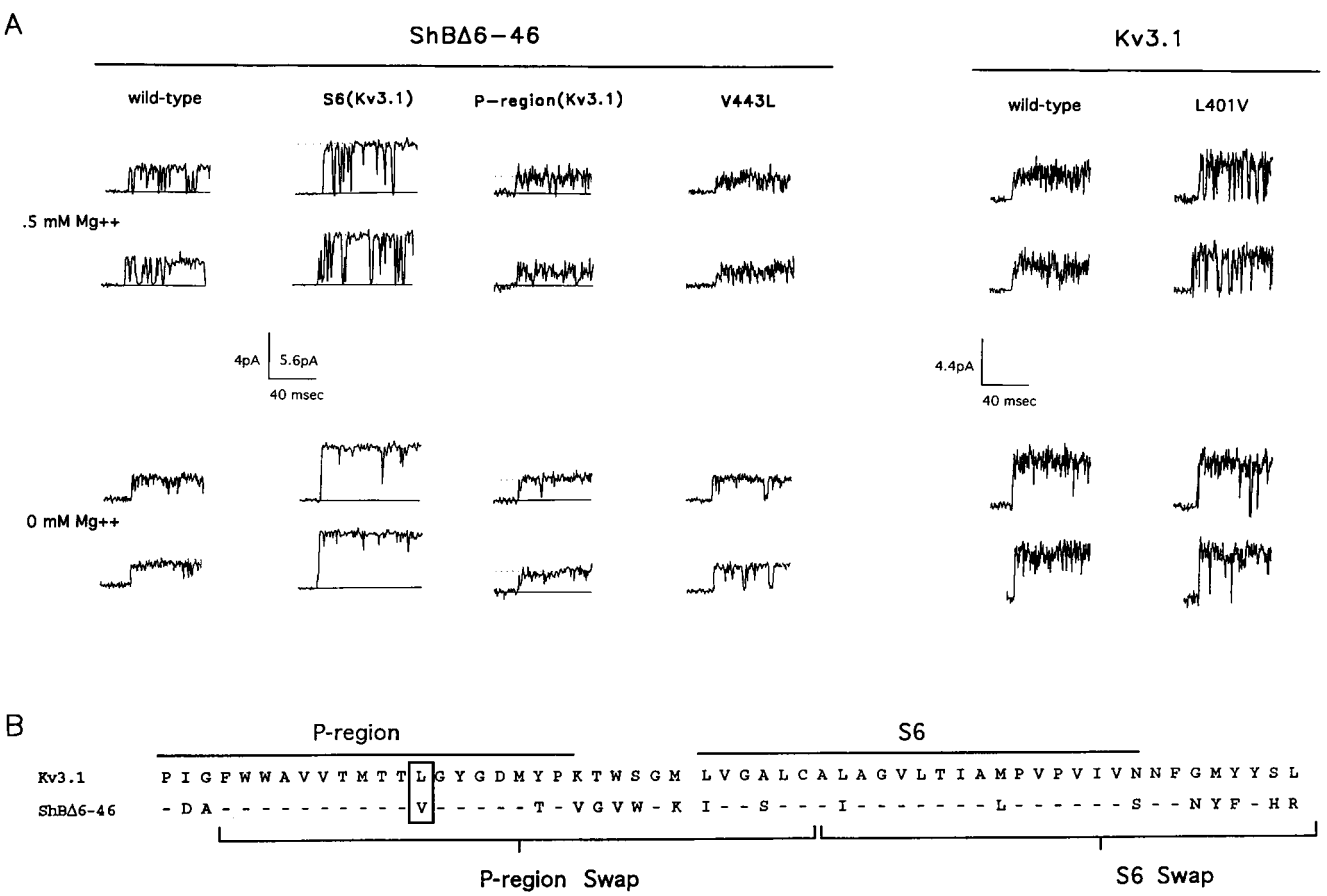

FIGURE 3 Mg^{2+} binding kinetics can be altered dramatically with mutations of a single residue in the P-region. (*A*) Transplantation of S6 from Kv3.1 into ShBΔ, ShBΔ[S6(Kv3.1)]) increases single-channel current but does not alter Mg^{2+} binding kinetics. Transplantation of the P-region from Kv3.1 into ShBΔ, ShBΔ[P-region(Kv3.1)] and the point mutation ShBΔ(V443L) convert the slow block of ShBΔ to fast Mg^{2+} blocking kinetics similar to those of Kv3.1. Mg_i^{2+} caused a decrease in mean single-channel current amplitude and increased open-channel noise. For ShBΔ(V443L) mean single-channel current amplitude decreases from 2.50 ± 0.03 pA (n = 2) to 1.54 ± 0.01 pA (n = 3), and open-channel noise increases from 0.17 ± 0.01 pA to 0.34 ± 0.01 pA in the presence of internal Mg^{2+}. The converse point mutation Kv3.1(L401V) converts the fast block of Kv3.1 to slow blocking kinetics characteristic of ShBΔ, with fully resolved Mg^{2+} binding and unbinding events. Mg_i^{2+} reduced mean open time from 18.12 ms (n = 1) to 2.35 ± 0.09 ms (n = 5). Kv3.1, ShBΔ, and the P-region chimera currents were reduced by 61.9%, 23.7%, and 44.1%, respectively, by 0.5 mM Mg^{2+}. A pair of traces is shown for each channel. The pipette (external) solution is 100 mM K^+ and the step potential is +160 mV. The scale bar is 4 pA and 40 ms for all ShBΔ channels, except for ShBΔ[S6(Kv3.1)], where the scale bar is 5.6 pA and 40 ms. The scale bar is 4.4 pA and 40 ms for all Kv3.1 channels. (*B*) Sequence alignment of the P-region through S6 of Kv3.1 and ShBΔ. Regions swapped from Kv3.1 into ShBΔ are underlined. Boxed residues are residues that were mutated.

Kv3.1(L401G) expressed at levels that were too low for patch-clamp experiments (data not shown). Mutation of a nearby conserved polar residue Kv3.1(T399S), analogous to a mutation that alters internal TEA blockade of ShBΔ (Yellen et al., 1991), had no effect on Mg^{2+} block at either the macroscopic or single-channel level (data not shown).

Kinetic analysis of magnesium block of Kv3.1

Because ShBΔ and Kv3.1(L401V) appeared identical in their block by Mg^{2+}, the remainder of the experiments focused on Mg^{2+} block of Kv3.1 and Kv3.1(L401V), because their single-channel conductances are twice that of ShBΔ, which simplifies single-channel analysis. To quantitate the rates of Mg^{2+} binding and unbinding to Kv3.1, which were too fast to resolve blocking and unblocking events, the technique of amplitude distribution analysis was used (Yellen, 1984a). This approach relies on the assumption that the channel fluctuates between two states of known conductance and that the fluctuations obey a Poisson process. Fig. 4 *A* shows representative single-channel traces used for the analysis. Because the Mg^{2+}-independent open-channel noise was significant, β-functions were convolved with a Gaussian distribution that described the open-channel noise in the absence of internal Mg^{2+}. The β-parameters of the convolved function were then fit to the amplitude distribution of single-channel events in the presence of internal Mg^{2+}. The fits were good (Fig. 4 *A*, *solid line*) and quite sensitive to alterations in blocking rates (Fig. 4 *A*, *dashed lines*). To optimize the analysis, 0.1 mM internal Mg^{2+} was used at +120 and +140 mV, and 0.5 mM internal Mg^{2+} was used at +80 and +100 mV, maximizing the block-induced open-channel noise (Fig. 5). All measurements were made in external Na_o^+ with 0 mM K_o^+.

The rate constants obtained from the amplitude distribution analysis were used to calculate K_i values, and these were compared with K_i values measured from macropatches. For +80 and +100 mV the K_i values calculated from the single-channel amplitude distribution analysis were (in mM) 0.81 ± 0.03 (n = 4) and 0.56 ± 0.06 (n = 7), respectively. K_i values measured from macropatches at these voltages were (in mM) 0.96 ± 0.06 (n = 3) and 0.53 ± 0.06 (n = 3), for +80 and +100 mV, respectively, indicating that the single-channel amplitude distribution analysis accounts well for the macroscopic block.

Kinetic analysis of magnesium binding for Kv3.1(L401V)

To obtain Mg^{2+} binding and unbinding rates for Kv3.1(L401V) channels, dwell-time histograms were made by using events acquired in the absence and presence of internal Mg^{2+}. In the presence of 0.5 mM Mg_i^{2+}, both open- and closed-time distributions were fit well by single exponentials (Fig. 4 *B*). In 0 mM Mg^{2+}, however, the open-time

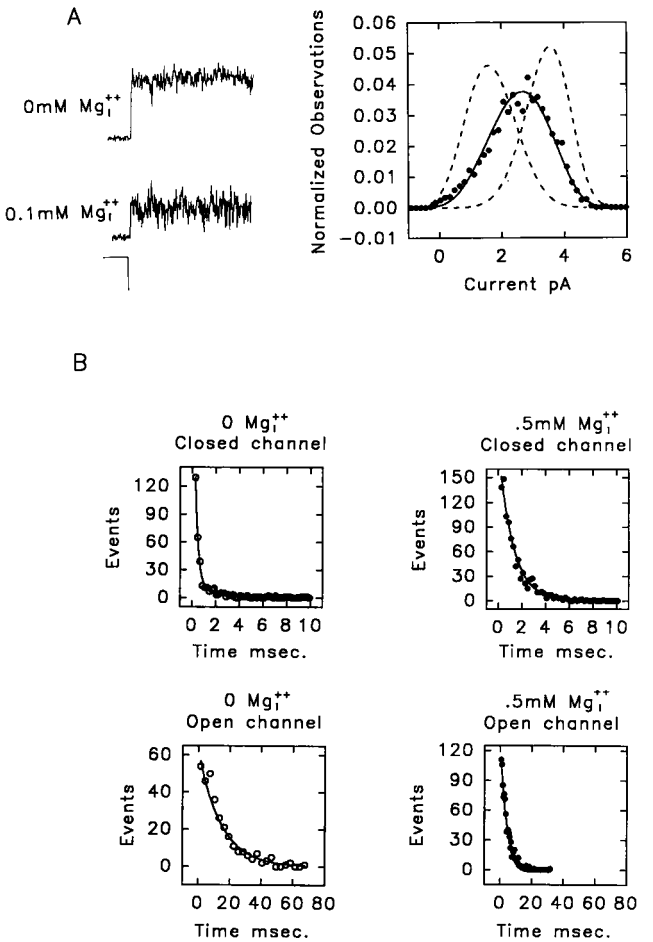

FIGURE 4 Single-channel magnesium blocking rates of Kv3.1 and Kv3.1(L401V) in 100 mM Na_o^+. (*A*) 0.1 mM internal Mg^{2+} (lower trace) decreases mean single-channel amplitude and increases noise relative to 0 Mg^{2+} control (upper trace) for Kv3.1. An amplitude histogram of open-channel noise is fitted with a β function that has been convolved with a Gaussian fit to the open-channel noise in the absence of internal Mg^{2+} (see Materials and Methods). Solid line indicates best fit 13,500 s^{-1} on rate and 17,000 s^{-1} off rate. Dashed lines indicate fits when either the on rate or the off rate is increased by a factor of 2. The step potential is +140 mV. Scale bars are 20 ms and 2 pA. (*B*) Dwell-time histograms for Kv3.1(L401V) in the absence and presence of internal Mg^{2+}. All fits are single exponentials, except for 0 Mg^{2+} closed times, in which two exponentials were required. Time constants are 0.31 ± 0.02 ms (n = 5) and 2.06 ± 1.49 ms (n = 3) for 0 Mg^{2+} closed channel, 1.01 ± 0.41 (n = 8) for 0.5 mM Mg^{2+} closed channel, 15.70 ± 2.38 (n = 7) for 0 Mg^{2+} open channel, and 4.31 ± 0.16 (n = 8) for 0.5 mM Mg^{2+} open channel. The step potential is +100 mV.

distribution was fit well by a single exponential, and the closed-time distribution required two exponentials (Fig. 4 *B*). This is consistent with the channel having a single open state (τ = 15.7 ms), which can be terminated by one of three events: Mg^{2+} binding, or by transition to one of two Mg^{2+}-independent closed states, C_{fast}, which is short lived (τ = 0.31 ms), and C_{slow}, which is longer lived (τ = 2.06 ms).

Because in the presence of Mg^{2+} there is a closed state of duration (τ = 1.01 ms) similar to that of the C_{slow} state (measured in 0 mM Mg^{2+}), the Mg^{2+} closed-time histogram is contaminated by some C_{slow} closing events. This

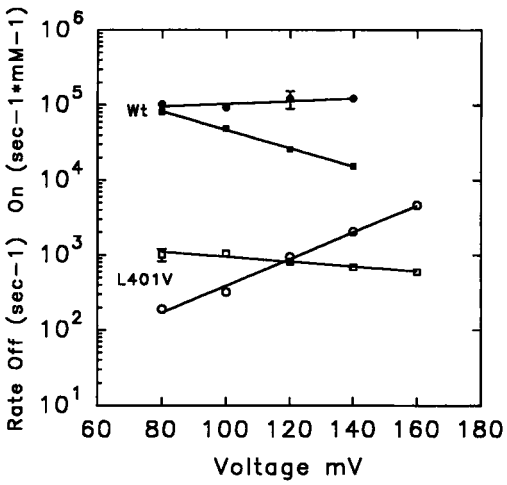

FIGURE 5 Voltage dependence of Mg^{2+} blocking kinetics for Kv3.1 and Kv3.1(L401V) in 100 mM Na^+ out. Lines are fits to the equation $k_{on} = k_{on(0\ mV)} * \exp(FVz\delta_{on}/RT)$ for the on rate and $k_{off} = k_{off(0\ mV)} * \exp -(FVz\delta_{off}/RT)$ for the off rate. δ_{on} and δ_{off} values are the electrical distance to the rate-limiting barrier for binding (on rate; ○, ●) and unbinding (off rate; □, ■), respectively. $k_{0\ mV}$ represents the rate with no applied voltage. For Kv3.1, δ_{on} and δ_{off} are 0.05 and 0.36, respectively. $k_{0\ mV}$ for on and off rates is 69,024 $s^{-1}mM^{-1}$ and 776,247 s^{-1}, respectively. For Kv3.1(L401V), δ_{on} and δ_{off} are 0.53 and 0.06, respectively. $k_{0\ mV}$ for on and off rates is 6.23 $s^{-1}mM^{-1}$ and 1445 s^{-1}, respectively. The majority of the voltage dependence of block is in the off rate for Kv3.1 and in the on rate for the mutant Kv3.1(L401V). The Mg^{2+} on rate for Kv3.1(L401V) was calculated as $k_{on\ Mg2+} = (1/\tau_{open\ Mg2+} - 1/\tau_{open\ 0\ Mg2+})/([Mg^{2+}])$, where $k_{on\ Mg2+}$ is the on rate for Mg^{2+}, $\tau_{open\ Mg2+}$ is the open time constant in the presence of Mg^{2+}, $\tau_{open\ 0\ Mg2+}$ is the open time constant in 0 Mg_i^{2+}, and $[Mg^{2+}]$ is the concentration of internal Mg^{2+}.

contamination appears to be small because the Mg^{2+} closed-time histogram was voltage dependent and remained monoexponential between +80 and +160 mV (Fig. 5), whereas both C_{fast} and C_{slow} in 0 Mg^{2+} were voltage-independent between +80 and +160 mV (data not shown), indicating that Mg^{2+} block events dominated the distribution. This observation is consistent with the calculation that even in the worst-case scenario, with the smallest depolarization used (to +80 mV, where the Mg^{2+} on rate should be slowest), the block rate was still eight times that of the closure to the C_{slow} state, minimizing contamination.

Voltage dependence of magnesium binding kinetics

For both Kv3.1 and Kv3.1(L401V), the off rate decreased with depolarization, suggesting that the majority of Mg^{2+} dissociations were in the inward direction (Fig. 5). However, there was a large difference in the magnitude of the single-channel Mg^{2+} binding kinetics for Kv3.1 and Kv3.1(L401V). At +80 mV the off rate was 100-fold faster, and the on rate 500-fold faster, for Kv3.1 than for Kv3.1(L401V). In addition, both δ_{on}, the electrical distance from the bulk solution to the rate-limiting barrier for Mg^{2+} entry, and δ_{off}, the electrical distance from the binding site to the rate-limiting barrier for Mg^{2+} exit, differed between Kv3.1 and Kv3.1(L401V) (compare the slopes of lines in Fig. 5). The major determinant for the voltage dependence of binding in Kv3.1 was in the off rate (δ_{off} = 0.36; δ_{on} = 0.05), suggesting that the rate-limiting energy barrier to Mg^{2+} entry lies near the cytoplasmic entrance to the pore in this channel. For Kv3.1(L401V) channels, on the other hand, most of the voltage dependence of binding was in the on rate (δ_{off} = 0.06; δ_{on} = 0.53), suggesting the opposite: that the rate-limiting barrier to Mg^{2+} entry is electrically close to the binding site.

The depth of the binding site in the electric field ($\delta = \delta_{on} + \delta_{off}$) was 0.18 deeper in the electric field for Kv3.1(L401V). The simplest explanation is that, as with ShBΔ in Na_o^+ (Fig. 2 *A*), the Mg^{2+} ion-binding site is located deeper in the pore for Kv3.1(L401V) than for Kv3.1 (Fig. 8 *A*).

The voltage dependence of macroscopic blocking affinity of Kv3.1 (δ = 0.40) and ShBΔ (δ = 0.54) in external Na^+ agreed with that calculated from single-channel kinetics for Kv3.1 (δ = 0.41) and Kv3.1(L401V) (δ = 0.62), providing further evidence that single-channel kinetics can account for the macroscopic characteristics of block, and that the L401V mutation in Kv3.1 converts its Mg^{2+} block to that of ShBΔ.

Effect of external potassium on magnesium-binding kinetics of Kv3.1(L401V)

We examined the effect of external K^+ on Mg^{2+} block at the single-channel level. A quantitative determination could not be made for Kv3.1 because 100 mM external K^+ reduced Mg^{2+} block open-channel noise too much to permit the amplitude distribution analysis. We therefore studied Kv3.1(L401V), in which open and block events could be resolved in both Na_o^+ and K_o^+. External K^+ had two effects on Kv3.1(L401V): it shortened the closed time (from 2.30 ± 0.09 ms to 0.71 ± 0.07 ms) and lengthened the open time (from 0.42 ± 0.02 ms to 2.35 ± 0.09 ms) (Fig. 6).

To determine if, as observed with ShBΔ (Fig. 2 *A*), the voltage dependence of Mg^{2+} block was influenced by external K^+ and, if so, which rate constant was sensitive to K_o^+, Mg^{2+} binding kinetics of Kv3.1(L401V) were measured across a voltage range in both external Na^+ and K^+. As shown in Fig. 7, only the voltage dependence of the on rate (δ_{on}) was sensitive to external K^+. Substitution of K_o^+ with Na_o^+ changed δ_{on} from 0.33 to 0.53, while δ_{off} remained unchanged. This change in the δ_{on} can account for the different voltage dependence of Mg^{2+} binding in K_o^+ versus Na_o^+ for ShBΔ in Fig. 2 *A*.

These results are consistent with the existence of, first, an external K^+ site outside the electric field, the occupancy of which decreases the dwell time of Mg^{2+} in its binding site by repulsion, as has been observed for inward rectifiers (Matsuda, 1991), and second, a deep site, the occupancy of which by K^+ interferes with Mg^{2+} access to its binding site (see Discussion).

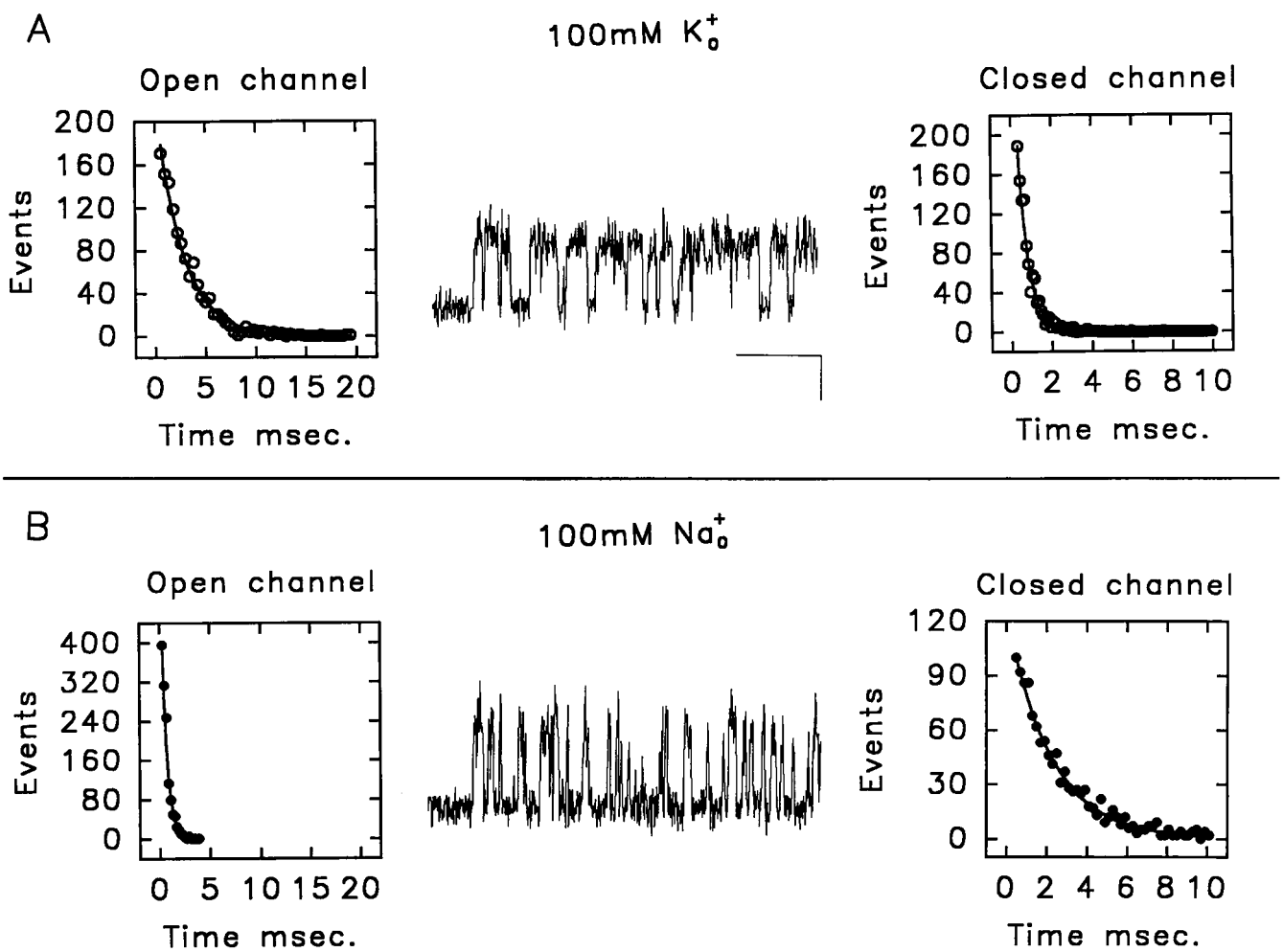

FIGURE 6 Influence of external K^+ on internal Mg^{2+} binding kinetics for Kv3.1(L401V). External K^+ has two effects on the mutant. The on rate is slowed by a factor of 6, and the off rate is increased by a factor of 2.5. (*A*) With 100 mM K_o^+ mean open time is 2.35 ± 0.09 ms and mean closed time is 0.71 ± 0.07 ms (n = 5). (*B*) With 100 mM Na_o^+ mean open time is 0.42 ± 0.02 ms and mean closed time is 2.30 ± 0.09 ms (n = 5). Step potential is +160 mV and internal Mg^{2+} is 0.5 mM. Scale bars are 10 ms and 2 pA for *A* and *B*.

DISCUSSION

Our results show that internal Mg^{2+} blocks both Kv3.1 and ShBΔ K^+ channels, with Kv3.1 having higher affinity and faster blocking kinetics than ShBΔ. We expect the fast block of Kv3.1 to be physiologically relevant. In cultured rat central neurons, free internal Mg^{2+} concentrations have been shown to vary from 0.5 mM to 12 mM (Brocard et al., 1993). This much internal Mg^{2+} would cause extensive block of Kv3.1 channels at 0 to +40 mV (see Fig. 2 *A*) during the action potential overshoot. The fact that the Mg^{2+} binding kinetics of Kv3.1 are faster than the rising phase of the action potential means that block could increase both the action potential amplitude and duration and, thus, increase the amount of neurotransmitter released at the nerve terminal.

For both Kv3.1 and ShBΔ, the mechanism of block appears to be due to binding of the Mg^{2+} ion to a site located deep within the permeation pathway, similar to what has been observed in other K^+ channels (Ludewig et al., 1993; Lu and MacKinnon, 1994; Lopatin et al., 1994; Yang et al., 1995). Transplantation of the P-region of Kv3.1 into ShBΔ conferred rapid block, characteristic of Kv3.1, on ShBΔ. The alteration of Mg^{2+} binding kinetics was attributed to a single amino acid residue L401 of Kv3.1 and its analog V443 in ShBΔ, with leucine conferring fast block and valine conferring slow block in both channels. Quantitation of the blocking kinetics indicated that the entry and exit rates of Mg^{2+} from its binding site were two orders of magnitude faster for Kv3.1 than for Kv3.1(L401V). This is a remarkable effect, given that leucine and valine differ by only a methylene group. Transplantation of S6 from Kv3.1 into ShBΔ, which has been shown to affect K^+ conductance (Lopez et al., 1994; Taglialatela et al., 1994a) and the Ba_i^{2+} on rate (Isacoff et al., 1993), however, did not appear to be important for Mg^{2+} binding in these channels. This suggests that the barriers to entry into the pore from the cytoplasm may be the same for K^+ and Ba^{2+}, but are different for Mg^{2+}.

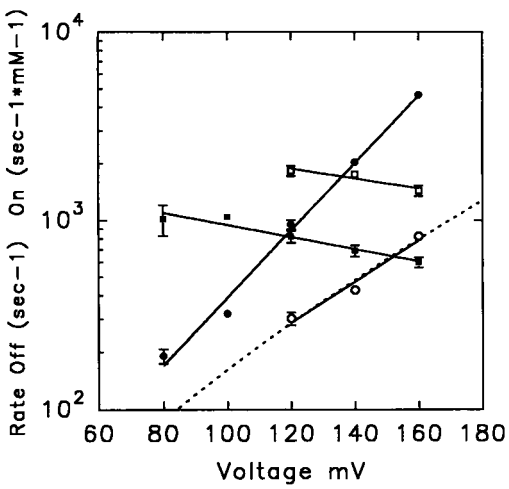

FIGURE 7 Voltage dependence of rate constants for Kv3.1(L401V) in 100 mM K_o^+ (○, □) and 100 mM Na_o^+ (●, ■). On rates are circles and off rates are squares. Solid lines are fits to the data as in Fig. 5. Switching from Na_o^+ to K_o^+ did not change δ_{off} (0.10 and 0.08), but δ_{on} decreased from 0.53 to 0.32. The dashed line represents the fit of our model for the apparent Mg^{2+} on rate to the data [The values for $k_{onMg2+0\ mV}$ and $\delta_{on\ Mg2+}$ were held constant at 6,230 $s^{-1}M^{-1}$ and 0.53, respectively (values obtained from Fig. 5) and $k_{onK+0\ mV}/k_{offK+}$ and δ_{onK+} were the free parameters]. $k_{offK+}/k_{onK+0\ mV}$ was 301 mM and δ_{onK+} was 0.45.

The result that the P-region and not S6 is important for internal Mg^{2+} block of voltage-gated K^+ channels is in stark contrast to what is observed in the inward rectifiers. In inward rectifiers it has been shown that M2, the structural homolog of S6 in voltage-gated K^+ channels, and residues C-terminal to M2, but not the P-region, play a role in internal Mg^{2+} binding (Wible et al., 1994; Lu and Mackinnon, 1994, 1995; Yang et al., 1995).

The mutation Kv3.1(L401V), shown earlier to leave K^+/Rb^+ selectivity unaltered (Aiyar et al., 1994), also left the channel essentially wild type in conductance and K^+/Na^+ selectivity. These results indicate that this substitution does not dramatically disrupt the pore, even though it substantially altered the voltage dependence and kinetics of Mg^{2+} block. The large and specific effect on Mg^{2+} block that we observe with a conservative mutation, combined with the evidence that the contrary substitution ShBΔ(V443L) has the reverse effect, is consistent with a direct effect of this residue on the energetics of Mg^{2+} movement in the pore.

What does the leucine at position 401 of Kv3.1 do to magnesium binding?

Cysteine scanning mutagenesis, in conjunction with thiol reagent probing, has indicated that residue V443 in ShBΔ and its analog in Kv2.1 face the aqueous lumen of the pore (Lu and Miller, 1995; Pascual et al., 1995) and thus could influence Mg^{2+} block. Our observations that valine permits deeper penetration of Mg^{2+} into the pore [larger δ for Kv3.1(L401V) compared to Kv3.1 in Na_o^+] and that entry into and exit from the deep Kv3.1(L401V) binding site are slow could be explained if Mg^{2+} were able to squeeze, with difficulty, through a ring of valines at position 401, but not through a bulkier ring of leucines (Fig. 8 *A*). However, the ring of leucines is not so bulky as to provide a rate-limiting barrier to the passage of the more easily dehydrated K^+ ion, because mutation of 401 to valine did not alter single-channel K^+ conductance. Because the fast block of Kv3.1 was eliminated by the L401V mutation, the shallower wild-type binding site must be eliminated by the substitution, suggesting that leucine at this position contributes to the wild-type Kv3.1 binding pocket for Mg^{2+}. It is possible that, with leucine at position 401, the Mg^{2+} ion is partially coordinated by a ring of threonines at position(s) 397 and/or 400 (but not 399, because we find no effect on Mg^{2+} block with the mutation T399S) constituting the shallower binding site. When valine is at position 401, Mg^{2+} may move deeper into the pore and be partially coordinated by a ring of tyrosines that face the aqueous lumen (Lu and Miller, 1995) in the conserved GYG sequence. Internal TEA is

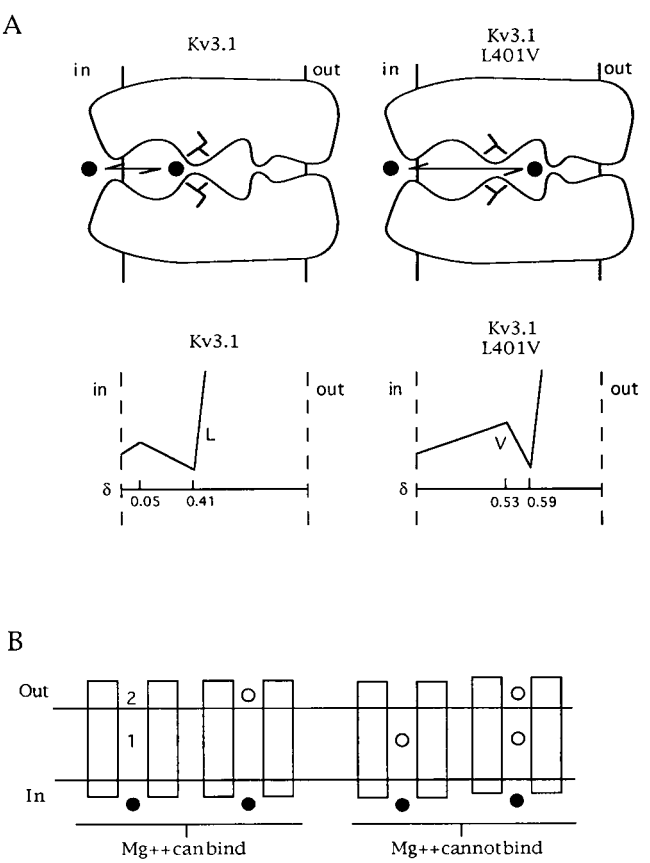

FIGURE 8 (*A*) Proposed model for the effect of mutation L401V. Decreasing the side-chain length by exchanging leucine for a valine lowers a prohibitive barrier for further movement in the pore. This allows Mg^{2+} to bind to a deeper site. Illustrative energy profiles of Kv3.1 and Kv3.1(L401V) showing qualitative barrier heights and well depths for Mg^{2+}. δ values represent the position in the membrane electric field of the binding site and the rate-limiting barrier for Mg^{2+} binding and unbinding. (*B*) Model of Mg^{2+} block of Kv3.1(L401V). ○, K^+ ions; ●, Mg^{2+} ions. The four possible states of the channel unbound by Mg^{2+} are shown.

thought to bind to a ring of threonines in ShBΔ analogous to position 399 of Kv3.1 (Yellen et al., 1991). The binding of TEA_i is weakly voltage dependent ($\delta = 0.15$), suggesting a sharp voltage drop in membrane potential (from 0.15 to 0.60) from positions T399 to Y403.

The Mg^{2+} off rate for Kv3.1 was very fast ($8 \times 10^5\ s^{-1}$ at 0 mV), indicating that Mg^{2+} binds weakly at the wild-type binding site. The on rate of Mg^{2+} block for Kv3.1 was also very fast ($7 \times 10^7\ M^{-1}\ s^{-1}$ at 0 mV), approaching the diffusion limit ($3 \times 10^8\ M^{-1}\ s^{-1}$) for Mg^{2+}, with a reaction capture radius of a K^+ ion with one water shell (Hille, 1992). This suggests that the barrier to entry of Mg^{2+} to its binding site in Kv3.1 is small and is consistent with the idea that although leucine at position 401 prevents deeper penetration of Mg^{2+} into the pore, it presents no barrier to entry into the weak binding site.

The identity of the residue at position 401 defined not only the apparent location of the Mg^{2+} binding site, and the height of the rate-limiting barrier for reaching and leaving the site, but also the apparent location of the barrier in the electric field. In Kv3.1 the majority of the voltage dependence of binding is in the off rate ($\delta_{off} = 0.36$), with little voltage dependence in the on rate ($\delta_{on} = 0.05$). For Kv3.1(L401V) the on rate carried the majority of the voltage dependence ($\delta_{on} = 0.53$), with little voltage dependence in the off rate ($\delta_{off} = 0.06$). These results suggest that the rate-limiting barrier to entry and exit of Mg^{2+} from the weak site in Kv3.1 is located close to the cytoplasmic entrance to the pore, whereas the rate-limiting barrier to entering the deep binding site of Kv3.1(L401V) (which may be valine itself, as argued above) is located near the binding site, deep within the pore (Fig. 8 *A*).

What does external potassium do to internal magnesium binding?

External K^+ decreased the affinity for Mg^{2+} binding in wild-type and mutant channels. This means that K_o^+ increases the off rate for Mg^{2+}, decreases the on rate for Mg^{2+}, or does a combination of both. K_o^+ decreased open channel noise in Kv3.1, indicating an increase in Mg^{2+} binding and/or unbinding rates. Because a decrease in block was accompanied by an increase in the binding kinetics, it must have been accompanied by an increase in the off rate (unbinding) of Mg^{2+}. This could be explained by simple repulsion between the two positively charged ions simultaneously occupying nearby sites in the pore. Such interactions are a natural consequence of multi-ion occupancy and have been proposed for other K^+ channels (Hille, 1992). The external K^+ ion appears to bind outside of the electric field, because the δ of Mg^{2+} binding in Kv3.1 was not altered by the addition of K_o^+. A similar effect was seen in the off rate of Mg^{2+} for Kv3.1(L401V). The off rate increased in the presence of external K^+, and the voltage dependence of Mg^{2+} unbinding (δ_{off}) was unaltered. A possible candidate for the external K^+ binding site is Y407 of Kv3.1, because mutation at the analogous position in RCK4 appears to alter internal Mg^{2+} binding indirectly through a change in an external K^+ binding site (Ludewig et al., 1993).

External K^+ decreased the δ of the Mg^{2+} binding site in both Kv3.1(L401V) and ShBΔ, but did not affect the δ of the Mg^{2+} binding site in Kv3.1. Our single-channel analysis of Kv3.1(L401V) showed that the decrease in δ with external K^+ resulted from a decrease in the voltage dependence of the on rate (δ_{on}) with no change in the voltage dependence of the off rate (δ_{off}). This could be explained in a number of ways. First, the binding of K_o^+ to an external binding site could alter the conformation of the pore and change the position of the binding site in the electric field. Second, external K^+ could change the voltage profile along the pore. However, because the δ_{off} for Mg^{2+} of Kv3.1(L401V) was unaltered by external K^+, these explanations seem unlikely. We propose an alternative explanation: the position of the Mg^{2+} ion binding site and the voltage profile may not be altered, and a K^+ ion may move in the field with a Mg^{2+} ion during block, thus changing the apparent δ_{on}. This proposition is appealing to us because it can be modeled and the model has some predictive value.

Model for the dependence of magnesium δ_{on} on external potassium for 1Kv3.1(L401V)

The slowing of the Mg^{2+} on rate (Figs. 6 and 7) and the decrease in the Mg^{2+} δ_{on} (Fig. 7) in Kv3.1(L401V) by external K^+ could be explained by a K^+ ion occupying a binding site in the electric field that prevents Mg^{2+} occupancy of its binding site. This would mean that in addition to the external K^+ binding site (site 2) that lies outside of the electric field, as discussed above, the channel has a deep K^+ site (site 1) that is located in the field (Fig. 8 *B*). When a K^+ ion is bound at site 1, Mg^{2+} cannot bind at its site because of the close proximity of the K^+ and Mg^{2+} binding sites, preventing simultaneous occupancy. In addition, Mg^{2+} cannot reach site 2 from the inside because of an impassable barrier that prevents Mg^{2+} from permeating the channel.

In this model, Mg^{2+} can arrive at the cytoplasmic entrance to the pore and find the Mg^{2+} unbound channel in one of four possible states of K^+ occupancy. If site 1 is occupied by K^+, then Mg^{2+} cannot bind (Fig. 8 *B*). Under the conditions of our experiments, at very depolarized voltages, site 1 is most likely to be occupied by K^+ originating from the internal solution, and the exit of K^+ from site 1 is most likely movement from site 1 to 2 (Hodgkin and Keynes, 1955). Because flux is single file, exit from site 1 could

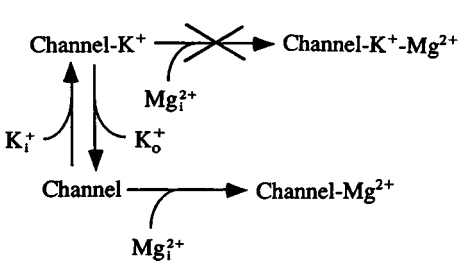

be rate-limited by the unbinding of K^+ from site 2; then, because site 2 lies outside of the electric field (as mentioned above), the off rate of K^+ from site 1 would be voltage independent. A simplified state diagram for Mg^{2+} block and unidirectional flow of K^+ into and out of site 1 is shown below (the states of the channel occupied at site 2 by K^+ have been ignored).

The solution for the apparent Mg^{2+} on rate for this scheme is shown below.

$$k_{\text{on Mg}^{2+}\text{app}} = k_{\text{on Mg}^{2+}} \times (\text{fraction of channels with site 1 empty}) \quad (2)$$

$$k_{\text{on Mg}^{2+}\text{app}} = \frac{k_{\text{on Mg}^{2+}\text{0 mV}} * \exp(FV2\delta_{\text{on Mg}^{2+}}/RT)}{1 + [K^+]_i * k_{\text{on K}^+\text{0 mV}} * \exp(FV\delta_{\text{on K}^+}/RT)/k_{\text{off K}^+}}. \quad (3)$$

This equation was used to fit the Mg^{2+} on rate of Kv3.1(L401V) in K_o^+ (Fig. 7, *dashed line*). [$k_{\text{on Mg2+0mV}}$ is the 0 mV on rate for Mg^{2+} measured in Na_o^+ (Fig. 5) (i.e., when sites 1 and 2 are rarely occupied by K^+); $\delta_{\text{on Mg2+}}$ is the electrical distance to the peak of the rate-limiting barrier for Mg^{2+} to enter its binding site from the inside, as measured in Na_o^+ (Fig. 5); $k_{\text{onK+0 mV}}$ is the K^+ on rate at 0 mV (free parameter); $k_{\text{offK+}}$ is the off-rate for K^+ (free parameter); and $\delta_{\text{onK+}}$ is the electrical distance to the peak of the rate-limiting barrier for K^+ to enter site 1 from the inside (free parameter).] The fit of this equation gives values for the free parameters, $\delta_{\text{onK+}} = 0.45$ and $k_{\text{offK+}}/k_{\text{onK+0 mV}} = 301$ mM, in accord with the idea that the K^+ binding site 1 is close enough to the Mg^{2+} binding site to exclude their simultaneous occupancy, with a significant occupancy of site 1 by K^+ at depolarized voltages with 100 mM K^+ internal. This model predicts that the apparent Mg^{2+} δ_{on} will be less at very depolarized voltages (as we observe) because of greater occupancy of site 1 by K^+. The reason the apparent Mg^{2+} δ_{on} is smaller with K_o^+ is that depolarization has two competing effects on the on rate of Mg^{2+}: directly increasing the Mg^{2+} on rate and indirectly decreasing it by increasing K^+ occupancy of site 1. In Na_o^+ a greater apparent δ_{on} is observed because in the absence of external K^+ at site 2 there is a reduced "lock-in" (Hodgkin and Keynes, 1955) of K^+ at site 1, thus decreasing occupancy by K^+ of site 1. In this model the δ of Mg^{2+} block for the wild-type channel, unlike the situation with valine at position 401, is insensitive to external K^+, because the voltage dependence of Mg^{2+} binding is in the off rate and not the on rate. A decrease in the Mg^{2+} δ_{on} from 0.05 (Fig. 5) in Kv3.1 would be impossible to detect and would not cause a significant change in the δ of the Mg^{2+} ion-binding site. Furthermore, Mg^{2+} may not compete with K^+ for its binding site, because the position of the Kv3.1 Mg^{2+} ion-binding site is located closer to the cytoplasmic entrance of the pore, where it might be unaffected by K^+ occupancy of site 1.

We thank O. Baker, A. Chamberlain, K. Glauner, H. P. Larsson, H. Lecar, L. Mannuzzu, J. Ngai, E. Reuveny, M. Siegel, and K. Zito for helpful discussions. Special thanks go to H. P. Larsson for help with the amplitude distribution analysis and A. Chamberlain for discussion of binding sites.

This work was supported in part by an American Heart Foundation, California Affiliate grant 94-216, the Mary Elisabeth Remie Endowment Fund for Epilepsy Research, and a junior faculty research grant from the University of California Committee on Research. REH was supported by a National Institutes of Health training grant (T32GM07232-18). This work was performed while EYI was a fellow of the Alfred P. Sloan Foundation, the Klingenstein Fund for Neuroscience, and the McKnight Endowment Fund for Neuroscience.

REFERENCES

Aiyar, J., A. Nguyen, K. Chandy, and S. Grissmer. 1994. The P-region and S6 of Kv3.1 contribute to the formation of the ion conduction pathway. *Biophys. J.* 67:2261–2264.

Aiyar, J., J. Withka, J. Rizzi, D. Singleton, G. Andrews, W. Lin, J. Boyd, D. Hanson, M. Simon, B. Dethlefs, C. Lee, J. Hall, G. Gutman, and K. Chandy. 1995. Topology of the pore-region of a K^+ channel revealed by the NMR-derived structures of scorpion toxins. *Neuron.* 15:1169–1181.

Armstrong, C., R. Swenson, and S. Taylor. 1982. Block of squid axon K^+ channels by internally and externally applied barium ions. *J. Gen. Physiol.* 80:663–682.

Brocard, J., S. Rajdev, and I. Reynolds. 1993. Glutamate-induced increases in intracellular free Mg^{2+} in cultured cortical neurons. *Neuron.* 11: 751–757.

Choi, K., C. Mossman, J. Aube, and G. Yellen. 1993. The internal quaternary ammonium receptor site of Shaker potassium channels. *Neuron.* 10:533–541.

Goldstein, S., D. Pheasant, and C. Miller. 1994. The charybdotoxin receptor of a *Shaker* K^+ channel: peptide and channel residues mediating molecular recognition. *Neuron.* 12:1377–1388.

Heginbotham, L., T. Abramson, and R. MacKinnon. 1992b. A functional connection between the pores of distantly related ion channels as revealed by mutant K^+ channels. *Science.* 258:1152–1155.

Heginbotham, L., Z. Lu, T. Abramson, and R. MacKinnon. 1994. Mutations in the K^+ channel signature sequence. *Biophys. J.* 66:1061–1067.

Heginbotham, L., and R. MacKinnon. 1992a. The aromatic binding site for tetraethylammonium ion on potassium channels. *Neuron.* 8:483–491.

Hidalgo, P., and R. MacKinnon. 1995. Revealing the architecture of a K^+ channel pore through mutant cycles with a peptide inhibitor. *Science.* 268:307–310.

Hille, B. 1992. Ionic Channels of Excitable Membranes. Sinauer Associates, Sunderland, MA.

Hodgkin, A., and R. Keynes. 1955. The potassium permeability of a giant nerve fibre. *J. Physiol. (Lond.).* 128:61–88.

Hoshi, T., W. Zagotta, and R. Aldrich. 1990. Biophysical and molecular mechanisms of Shaker potassium channel inactivation. *Science.* 250: 533–538.

Isacoff, E. Y., Y. N. Jan, and L. Y. Jan. 1991. Putative receptor for the cytoplasmic inactivation gate in the Shaker K^+ channel. *Nature.* 353: 86–90.

Isacoff, E., G. Lopez, Y. Jan, and L. Jan. 1993. A site near the transmembrane segment S6 of potassium channels interacts with barium ions. *Biophys. J.* 64:A226. (Abstr.)

Kubo, Y., T. Baldwin, Y. Jan, and L. Jan. 1993. Primary structure and functional expression of a mouse inward rectifier potassium channel. *Nature.* 362:127–133.

Kurz, L., R. Zuhlke, H. Zhang, and R. Joho. 1995. Side-chain accessibilities in the pore of a K^+ channel probed by sulfhydryl-specific reagents after cysteine-scanning mutagenesis. *Biophys. J.* 68:900–905.

Lopatin, A. N., E. N. Makhina, and C. G. Nichols. 1994. Potassium channel block by cytoplasmic polyamines as the mechanism of intrinsic rectification. *Nature.* 372:366–369.

Lopez, G. A., Y. N. Jan, and L. Y. Jan. 1994. Evidence that the S6 segment of the Shaker voltage-gated K^+ channel comprises part of the pore. *Nature.* 367:179–182.

Lu, Q., and C. Miller. 1995. Silver as a probe of pore-forming residues in a potassium channel. *Science.* 268:304–307.

Lu, Z., and R. MacKinnon. 1994. Electrostatic tuning of Mg^{2+} affinity in an inward-rectifier K^+ channel. *Nature.* 371:243–246.

Lu, Z., and R. MacKinnon. 1995. Probing a potassium channel pore with an engineered protonatable site. *Biochemistry.* 34:13133–13138.

Ludewig, U., C. Lorra, O. Pongs, and S. H. Heinemann. 1993. A site accessible to extracellular TEA^+ and K^+ influences intracellular Mg^{2+} block of cloned potassium channels. *Eur. Biophys. J.* 22:237–247.

MacKinnon, R., L. Heginbotham, and T. Abramson. 1990. Mapping the receptor site for charybdotoxin, a pore-blocking potassium channel inhibitor. *Neuron.* 5:767–771.

MacKinnon, R., and C. Miller. 1989. Mutant potassium channels with altered binding of charybdotoxin, a pore-blocking peptide inhibitor. *Science.* 245:1382–1385.

MacKinnon, R., and G. Yellen. 1990. Mutations affecting TEA blockade and ion permeation in voltage-activated K^+ channels. *Science.* 250: 276–279.

Matsuda, H. 1991. Effects of external and internal K^+ ions on magnesium block of inwardly rectifying K^+ channels in guinea pig heart cells. *J. Physiol. (Lond.).* 435:83–99.

Matsuda, H., A. Saigusa, and H. Irisawa. 1987. Ohmic conductance through the inwardly rectifying K^+ channel and blocking by internal Mg^{2+}. *Nature.* 325:156–159.

Neyton, J., and C. Miller. 1988a. Potassium blocks barium permeation through a calcium-activated potassium channel. *J. Gen. Physiol.* 92: 549–567.

Neyton, J., and C. Miller. 1988b. Discrete Ba^{2+} block as a probe of ion occupancy and pore structure in the high-conductance Ca^{2+}-activated K^+ channel. *J. Gen. Physiol.* 92:569–586.

Pascual, J. M., C. Shieh, G. Kirsch, and A. Brown. 1995. K^+ pore structure revealed by reporter cysteines at inner and outer surfaces. *Neuron.* 14:1055–1063.

Sambrook, J., E. Fritsch, and T. Maniatis. 1989. Molecular Cloning, 2nd Ed. Cold Spring Harbor Laboratory Press, Cold Spring Harbor, NY.

Slesinger, P., Y. Jan, and L. Jan. 1993. The S4–S5 loop contributes to the ion-selective pore of potassium channels. *Neuron.* 11:739–749.

Stanfield, P., N. Davies, P. Shelton, M. Sutcliffe, I. Khan, W. Brammer, and E. Conley. 1994. A single aspartate residue is involved in both intrinsic gating and blockage by Mg^{2+} of the inward rectifier, Irk-1. *J. Physiol. (Lond.).* 478:1–6.

Taglialatela, M., M. S. Champagne, J. A. Drewe, and A. M. Brown. 1994a. Comparison of H5, S6, and H5–S6 exchanges on pore properties of voltage-dependent K^+ channels. *J. Biol. Chem.* 269:13867–13873.

Taglialatela, M., J. A. Drewe, G. E. Kirsch, B. M. De, H. A. Hartmann, and A. M. Brown. 1993. Regulation of K^+/Rb^+ selectivity and internal TEA blockade by mutations at a single site in K^+ pores. *Pflugers Arch.* 423:104–112.

Taglialatela, M., B. A. Wible, R. Caporaso, and A. M. Brown. 1994b. Specification of pore properties by the carboxyl terminus of inwardly rectifying K^+ channels. *Science.* 264:844–847.

Yang, J., Y. N. Jan, and L. Y. Jan. 1995. Control of rectification and permeation by residues in two distinct domains in an inward rectifier K^+ channel. *Neuron.* 14:1047–1054.

Yellen, G. 1984a. Ionic permeation and blockade in Ca^{2+}-activated K^+ channels of bovine chromaffin cells. *J. Gen. Physiol.* 84:157–186.

Yellen, G. 1984b. Relief of Na^+ block of Ca^{2+}-activated K^+ channels by external cations. *J. Gen. Physiol.* 84:187–199.

Yellen, G., M. Jurman, T. Abramson, and R. MacKinnon. 1991. Mutations affecting internal TEA blockade identify the probable pore-forming region of a K^+ channel. *Science.* 251:939–942.

Yool, A., and T. Schwarz. 1991. Alteration of ionic selectivity of a K^+ channel by mutation of the H5 region. *Nature.* 349:700–704.

Wible, B., M. Taglialatela, E. Ficker, and A. Brown. 1994. Gating of inwardly rectifying K^+ channels localized to a single negatively charged residue. *Nature.* 371:246–249.

Woodhull, A. 1973. Ionic blockage of sodium channels in nerve. *J. Gen. Physiol.* 61:687–708.